

The role of cosmic rays on magnetic field diffusion and the formation of protostellar discs

Marco Padovani (LUPM – Montpellier)

in collaboration with

Daniele Galli (INAF-OAA – Firenze)

Patrick Hennebelle, Marc Joos (CEA – Saclay)

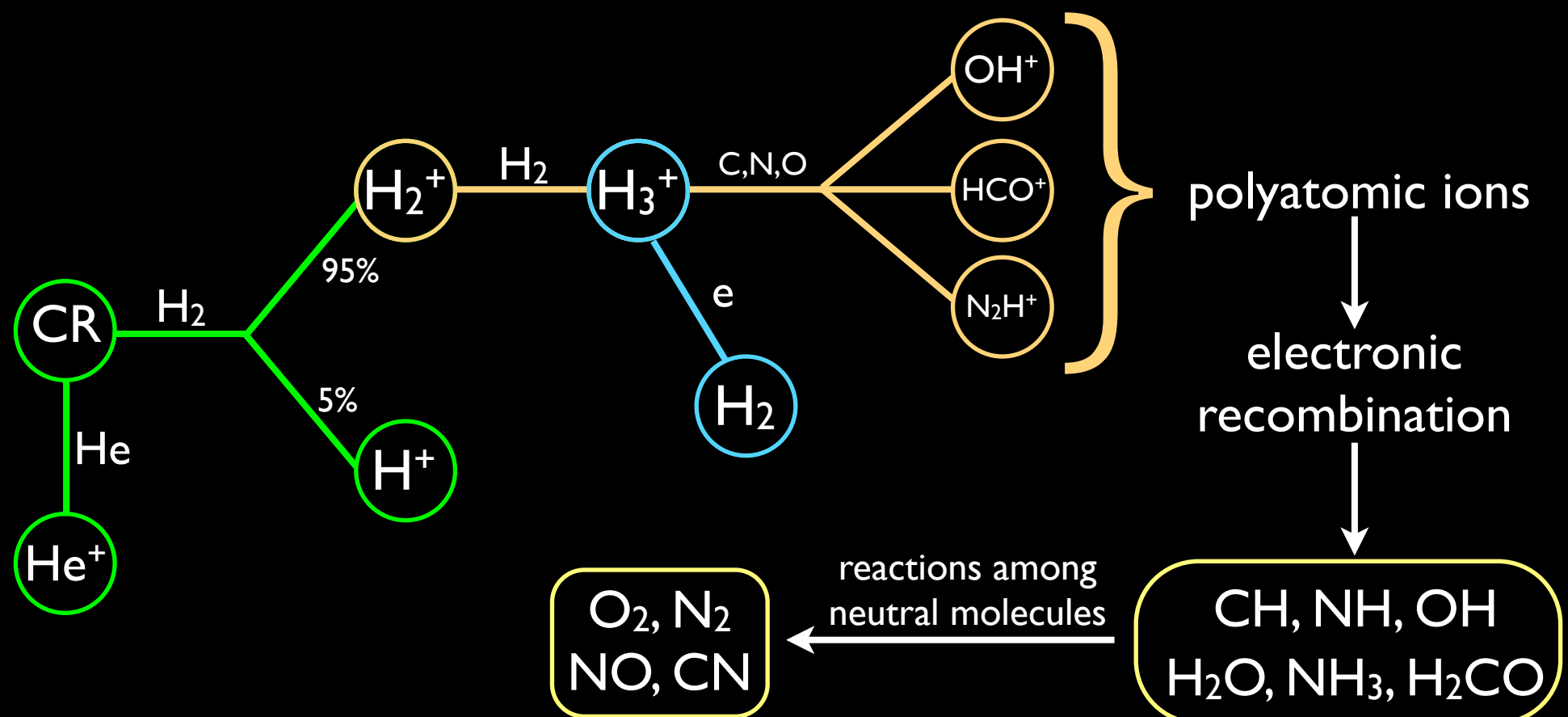
Benoît Commerçon (ENS – Lyon)

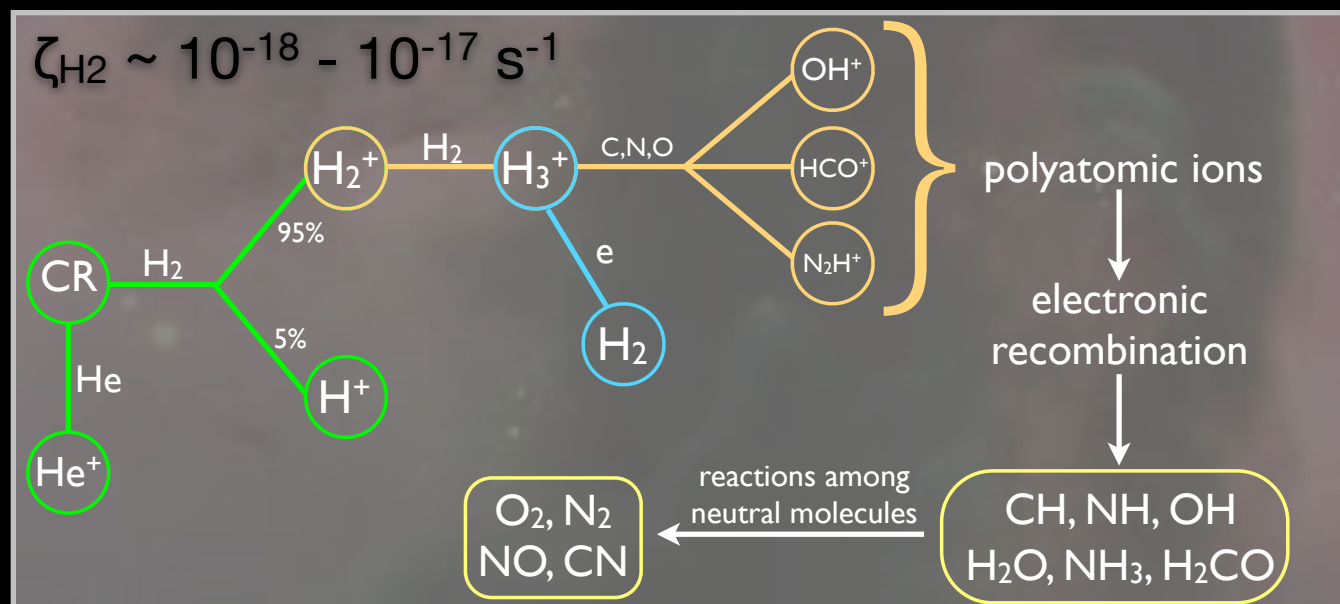
- Development of new telescopes with higher and higher resolution
- New observation techniques with consequent large data sets

- H₃⁺ : UKIRT, VLT-CRIRES — *Indriolo+ (2012)*
- OH⁺, H₂O⁺ : Herschel — *Neufeld+ (2010), Gerin+ (2010)*
- γ-ray emission : Fermi-LAT (CTA) — *Montmerle (2010)*
- magnetic field morphology : SMA, Planck (ALMA) — *Girart+ (2009)*

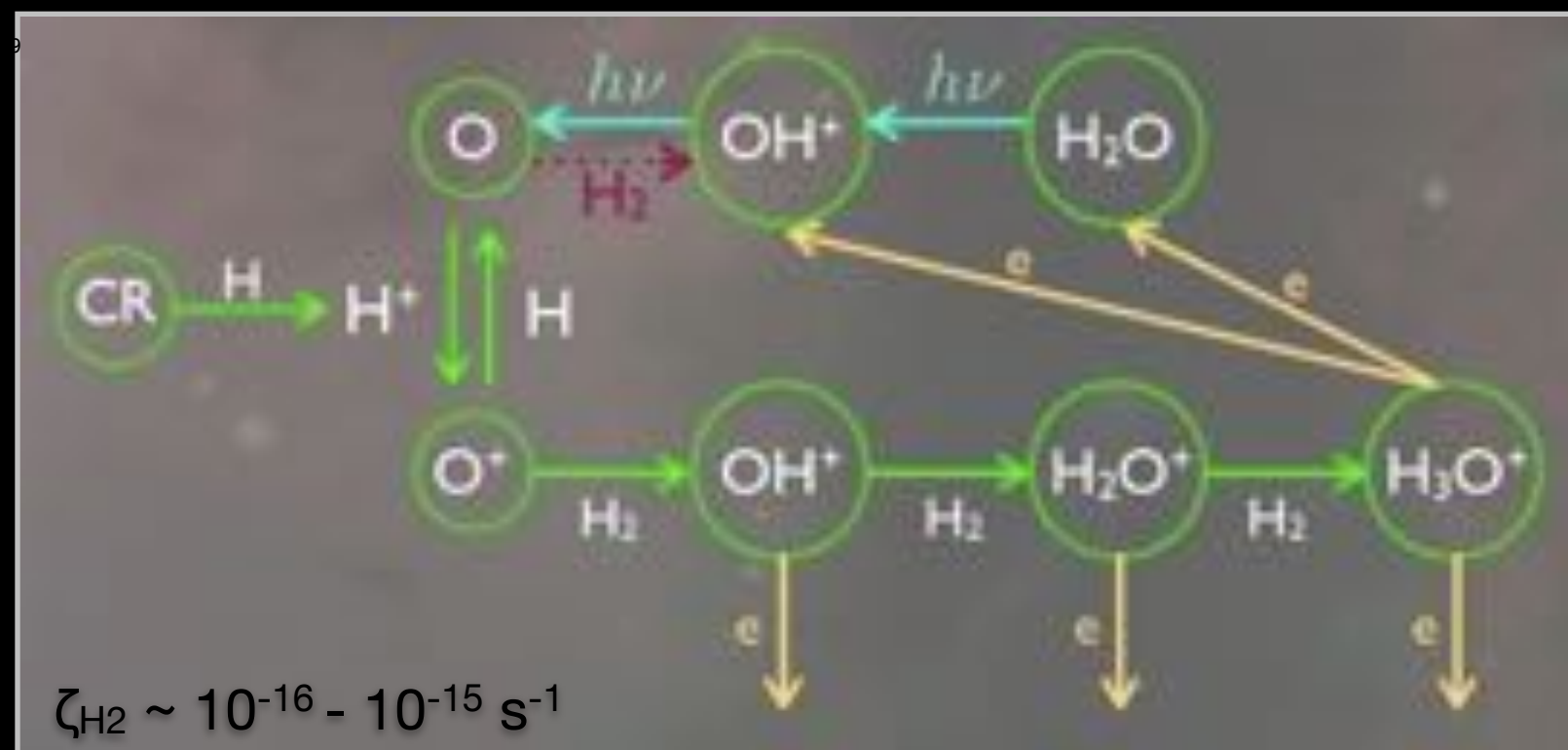
All these observations require a solid theoretical support. A detailed effort in the modelling of the CR spectrum, and more precisely of its low-energy tail, was missing as well as the integration of the models in chemical and numerical codes for interpreting observations.

- Diffuse clouds ($A_v \sim 1$ mag) → the UV radiation field is the principal ionising agent (photodissociation regions);
- Dense clouds ($A_v \gtrsim 5$ mag) → the ionisation is due to low-energy CRs ($E < 100$ MeV) and, if close to young stars, to soft X-rays ($E < 10$ keV).





Dense cores
(HCO^+ , DCO^+)
Caselli+ (1998)



Diffuse clouds
(OH , HD , NH)

Black & Dalgarno (1977),
Hartquist+ (1978), Black+ (1978),
van Dishoeck & Black (1986),
Federman+ (1996)
(H_3^+)
McCall+ (1993), Geballe+ (1999)
McCall+ (2003), Indriolo+ (2009, 2012)
(OH^+ , H_3O^+)
Neufeld+ (2010), Gerin+ (2010)

Main questions:

- origin of the CR flux that generates such a high ionisation rate (ζ_{CR}) in diffuse regions;
- how to reconcile these values with those ones measured in denser regions;

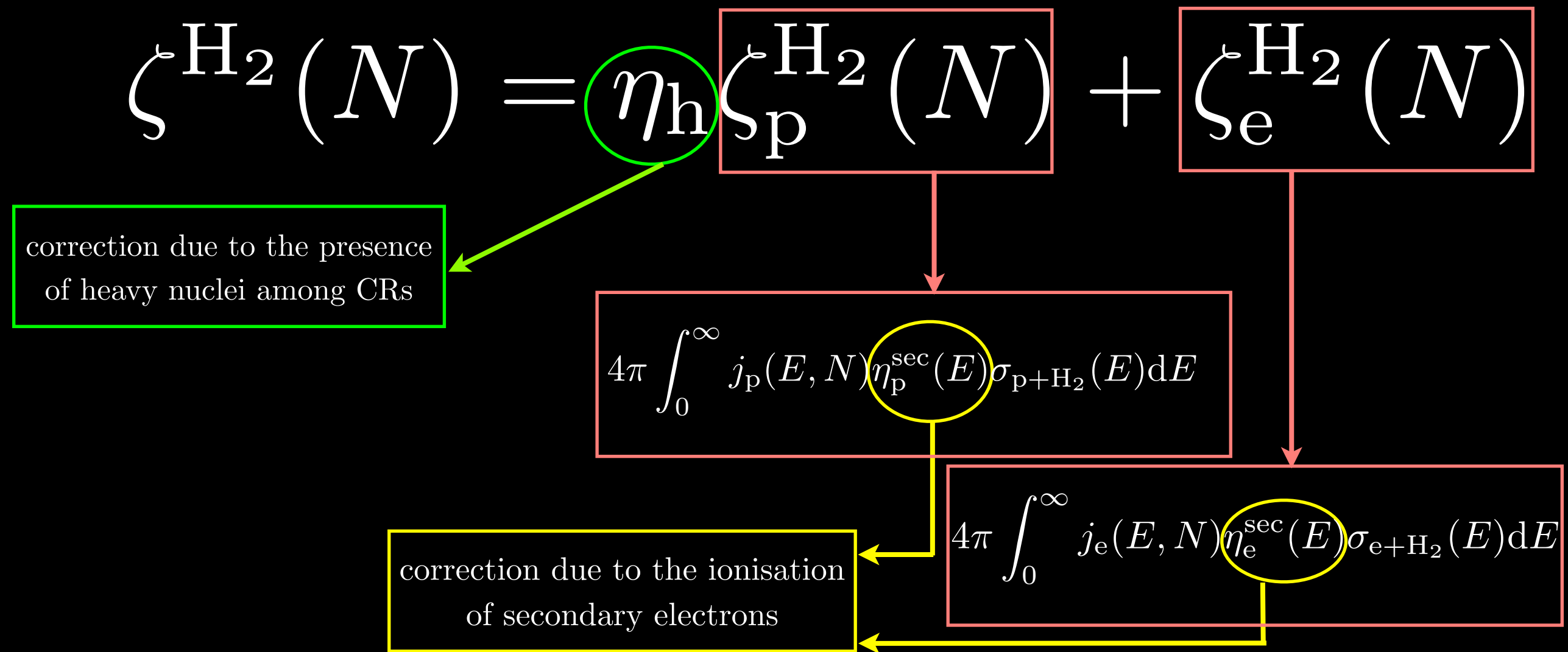
Different strategies approaching these problems:

- effects of Alfvén waves on CR streaming
 Skilling & Strong (1976); Hartquist+ (1978); Padoan & Scalo (2005);
 Everett & Zweibel (2011); Rimmer+ (2012); Morlino & Gabici (2014);
- magnetic mirroring and focusing
 Cesarsky & Völk (1978); Chandran (2000); **PM & Galli (2011,2013)**;
- possible low-energy CR flux able to ionise diffuse but not dense clouds
 Takayanagi (1973); Umebayashi & Nakano (1981); McCall+ (2003); **PM, Galli & Glassgold (2009)**

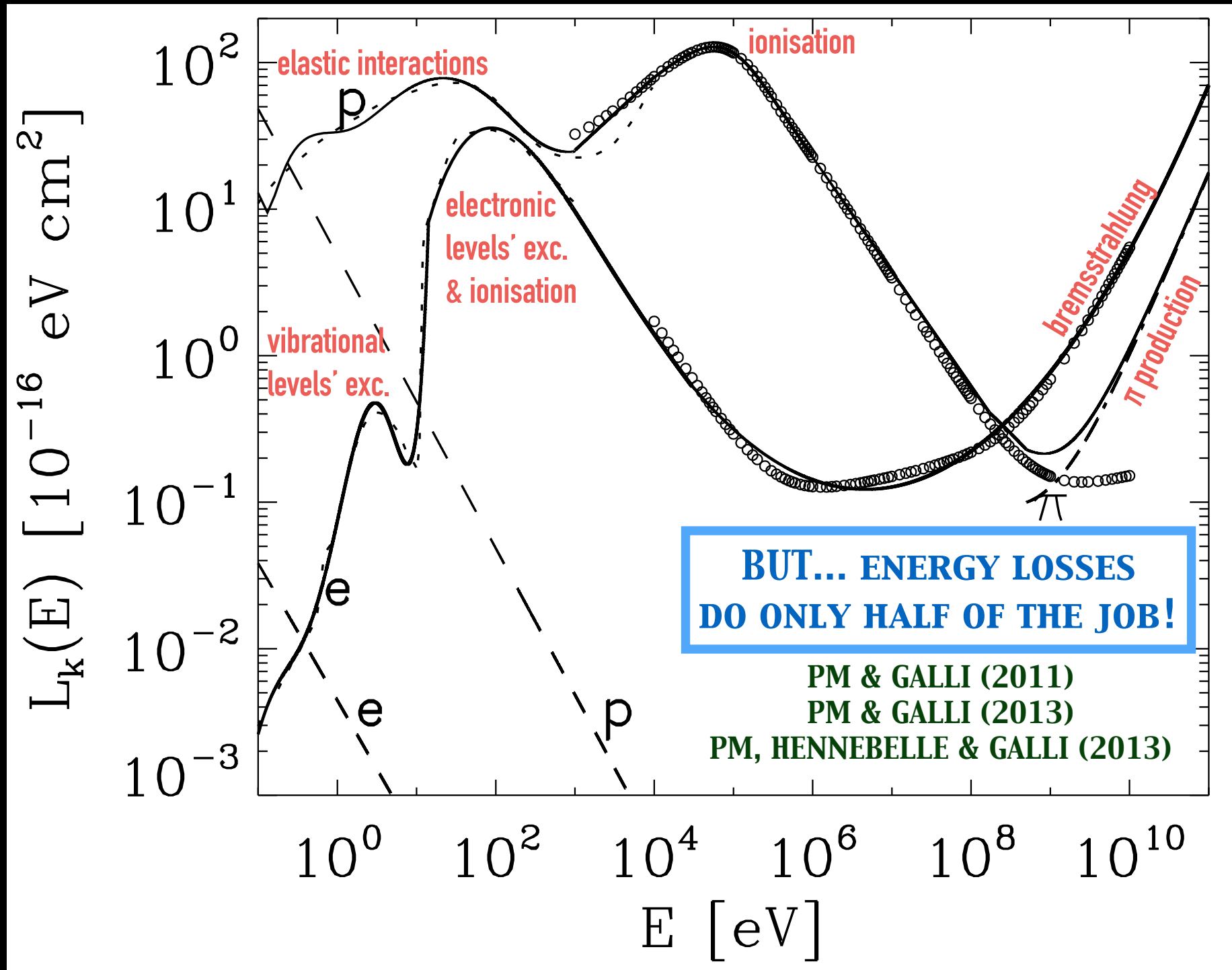
The story so far...

Theoretical model (PM, Galli & Glassgold 2009)

computing the variation of the ionisation rate due to cosmic rays, $\zeta_{\text{CR}} [\text{s}^{-1}]$, inside a molecular cloud, with the increasing of the column density, $N [\text{cm}^{-2}]$, of the traversed interstellar matter.



CR-proton and electron energy loss function



B

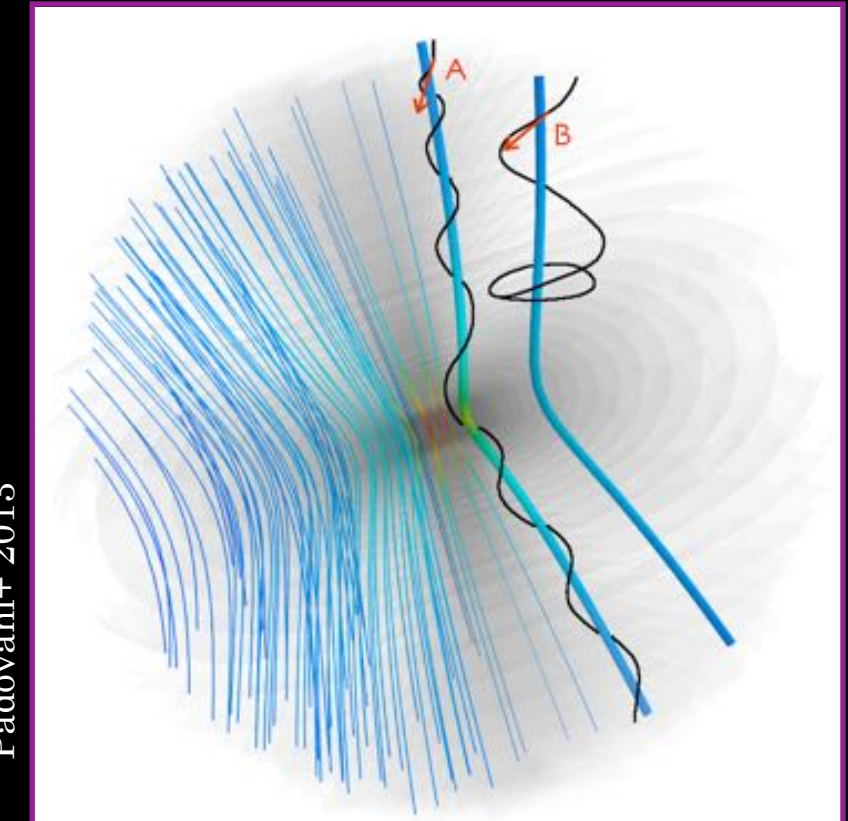
magnetic mirroring

bounces many CRs
out of the core

magnetic focusing

increases CR flux
in the core

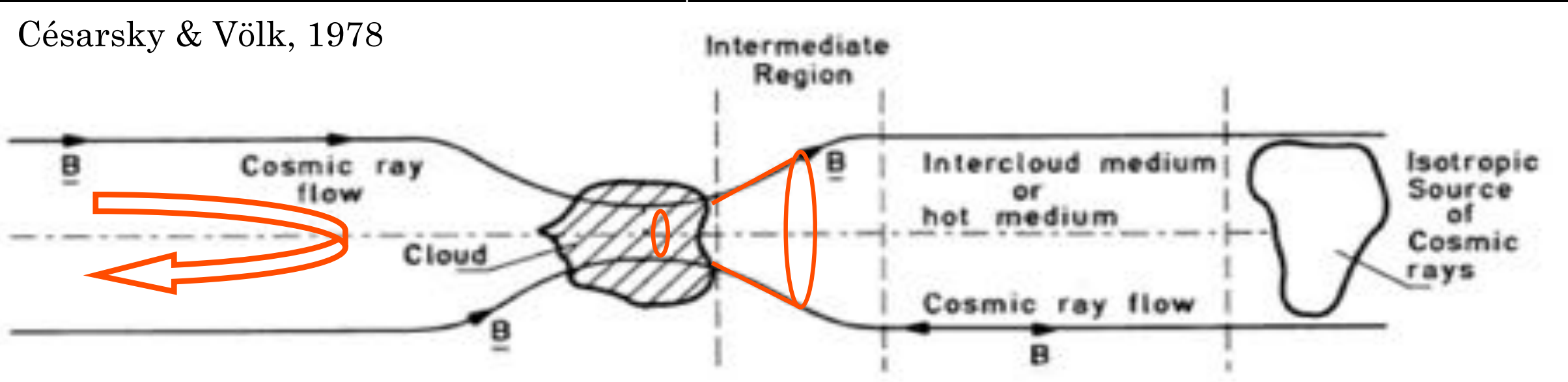
Padovani+ 2013



non-uniformity of the magnetic field

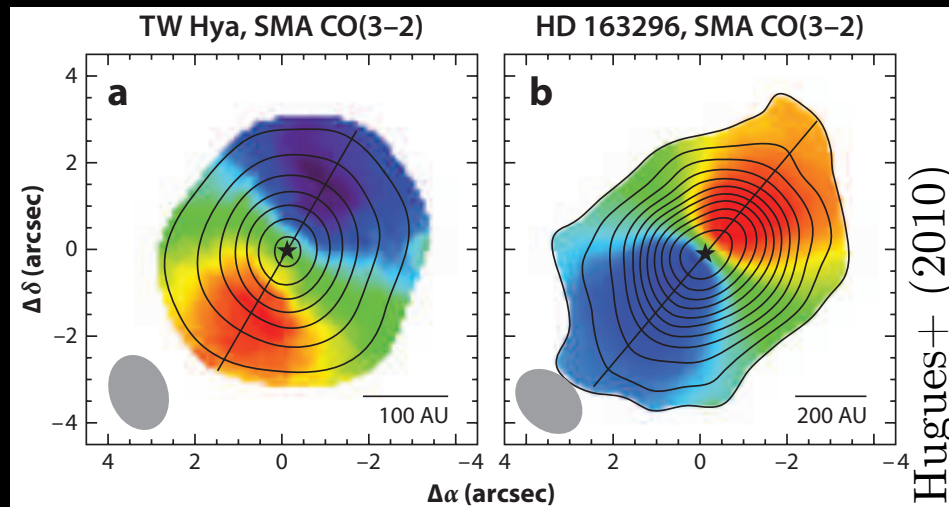
Césarsky & Völk, 1978

The Larmor radii of ionising CRs are smaller than typical sizes of Bok globules (~ 0.05 pc), dense cores ($\sim 1-5$ pc), and GMC (~ 25 pc).

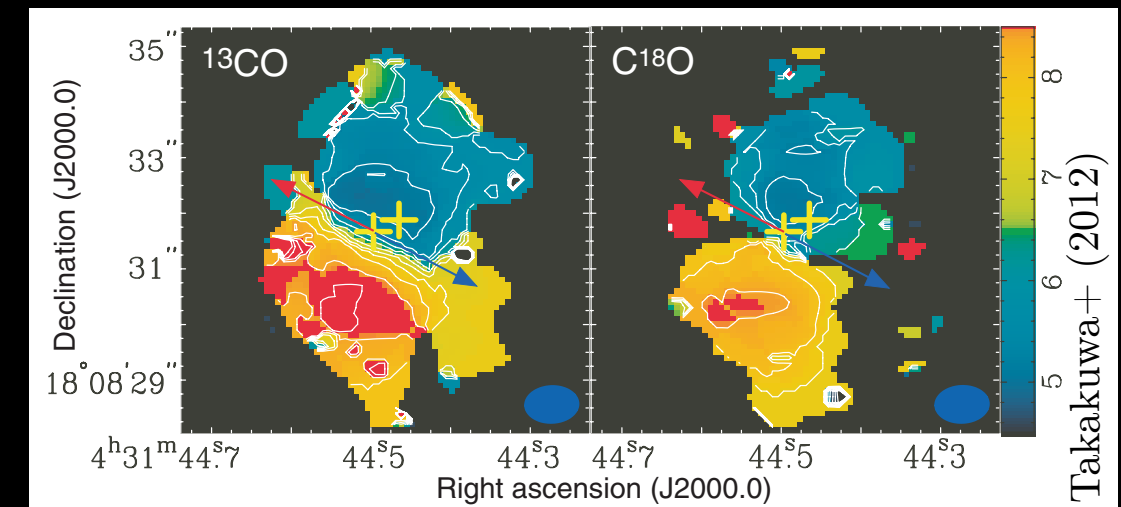


- Theoretical challenge: formation of protostellar discs.
- Magnetic fields entrained by collapsing cloud brake any rotational motion and prevents cloud's collapse (Galli+ 2006; Mellon & Li 2008; Hennebelle & Fromang 2008).

Observational evidence of the presence of discs

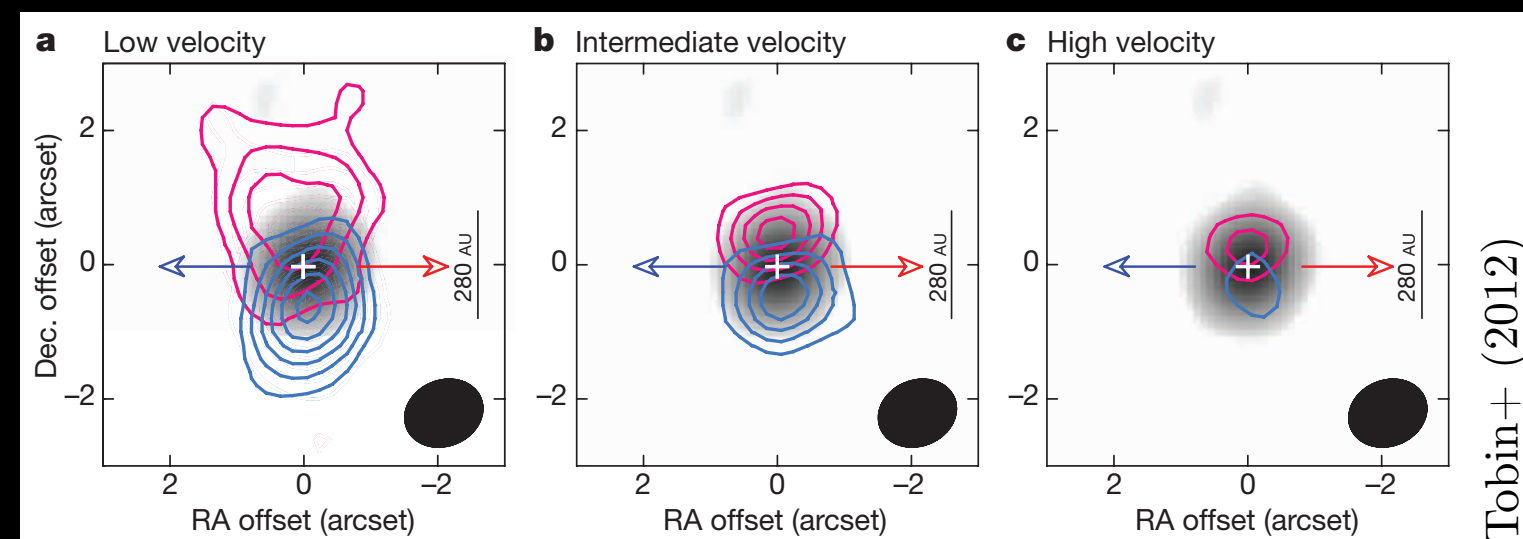


Class II YSO



Class I YSO

Class 0 YSO



- A number of possible solution to solve the magnetic braking
 - (i) non-ideal MHD effects (Shu+ 2006; Dapp & Basu 2010; Krasnopolksky+ 2011; Braiding & Wardle 2012)
 - (ii) misalignment between **B** and **J** (Hennebelle & Ciardi 2009; Joos+ 2012)
 - (iii) turbulent diffusion of **B** (Seifried+ 2012; Santos-Lima+ 2013; Joos+ 2013)
 - (iv) depletion of the infalling envelope anchoring **B** (Mellon & Li 2009; Machida+ 2011)

Numerical models : rotating collapsing core

Table 1. Parameters of the simulations described in the text (from Joos et al. 2012): mass-to-flux ratio, initial angle between the magnetic field direction and the rotation axis, time after the formation of the first Larson's core (core formed in the centre of the pseudo-disc with $n \gtrsim 10^{10} \text{ cm}^{-3}$ and $r \sim 10 - 20 \text{ AU}$), maximum mass of the protostellar core and of the disc. Last column gives information about the disc formation.

Case	λ	$\alpha_{\text{B,J}}$ [rad]	t [kyr]	M_\star [M_\odot]	M_{disc} [M_\odot]	Disc ?
A ₁	5	0	0.824	–	–	N
A ₂	5	0	11.025	0.26	0.05	N
B	5	$\pi/4$	7.949	0.23	0.15	Y
C	5	$\pi/2$	10.756	0.46	0.28	K
D	2	0	5.702	0.24	–	N
E	17	0	6.620	0.43	0.15	K

^a A disc with flat rotation curve is formed (Fig. 15 in Joos et al. 2012).

^b No significant disc is formed ($M_{\text{disc}} < 5 \times 10^{-2} M_\odot$).

^c A keplerian disc is formed (Fig. 14 in Joos et al. 2012).

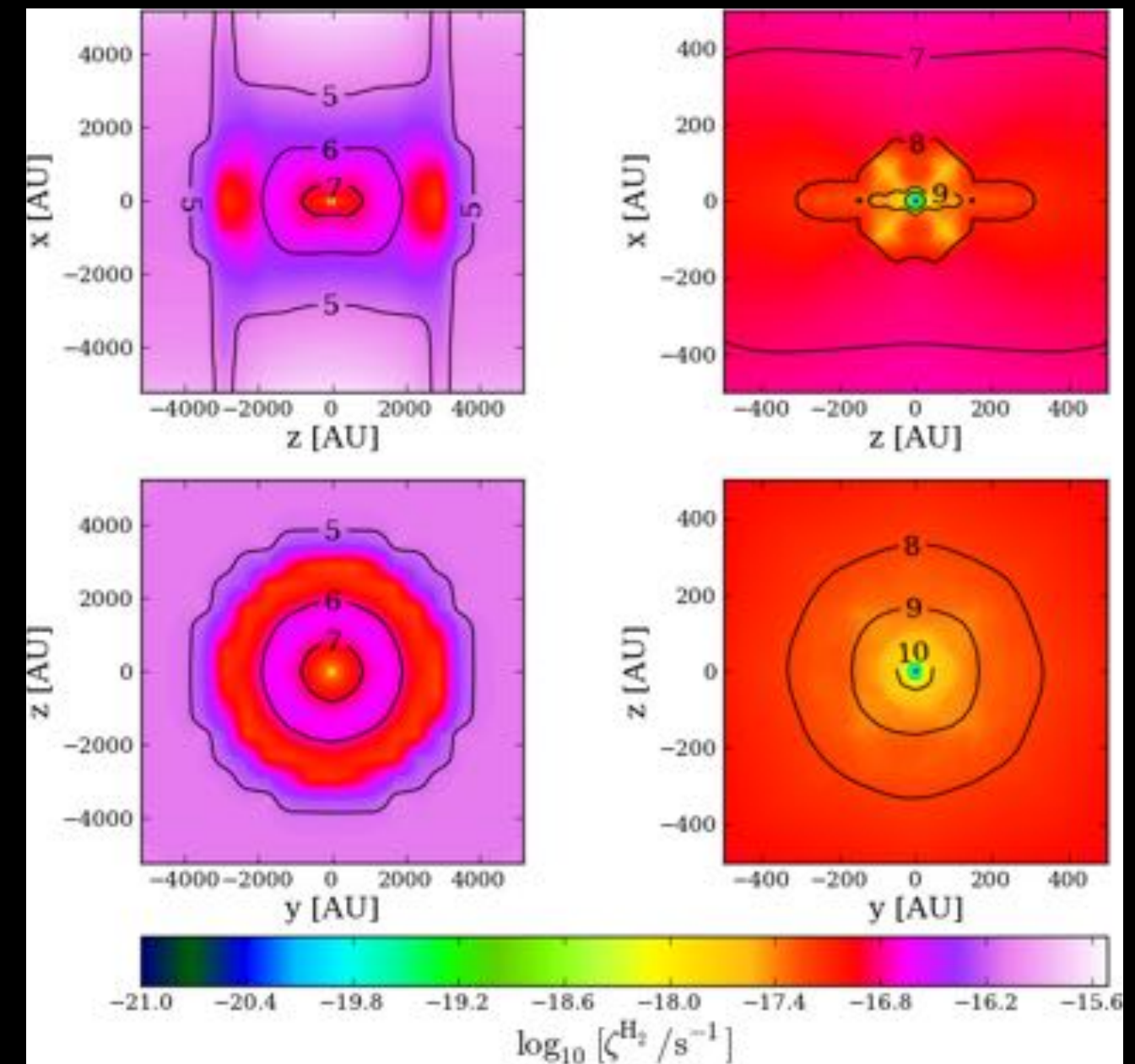
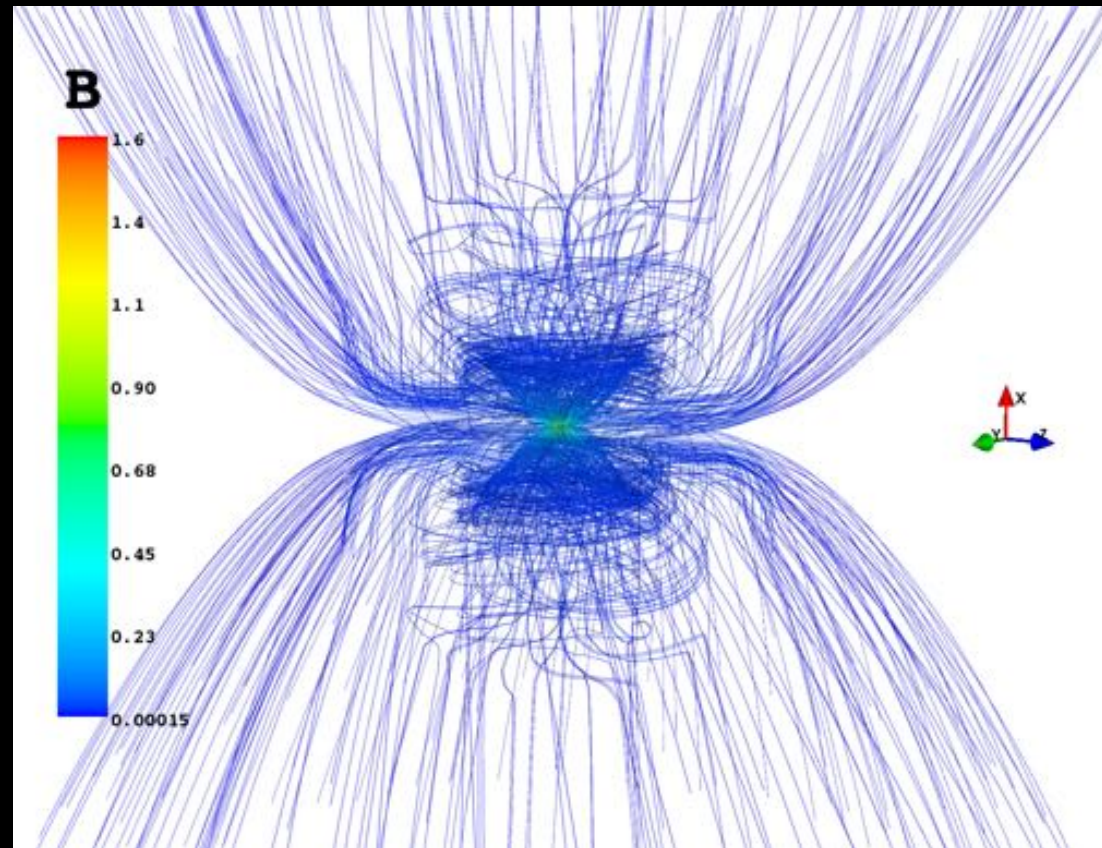
Numerical models : rotating collapsing core

Intermediate magnetisation $\lambda=5$

Aligned rotator (\mathbf{J}, \mathbf{B})=0

It is not possible to unravel magnetic from column-density effects, but both intervene on the decrease of ζ_{CR} . Deviations between iso-density contours and ζ_{CR} maps can be interpreted as due to magnetic imprints

Field lines in the inner 600 AU



Padovani+ 2013

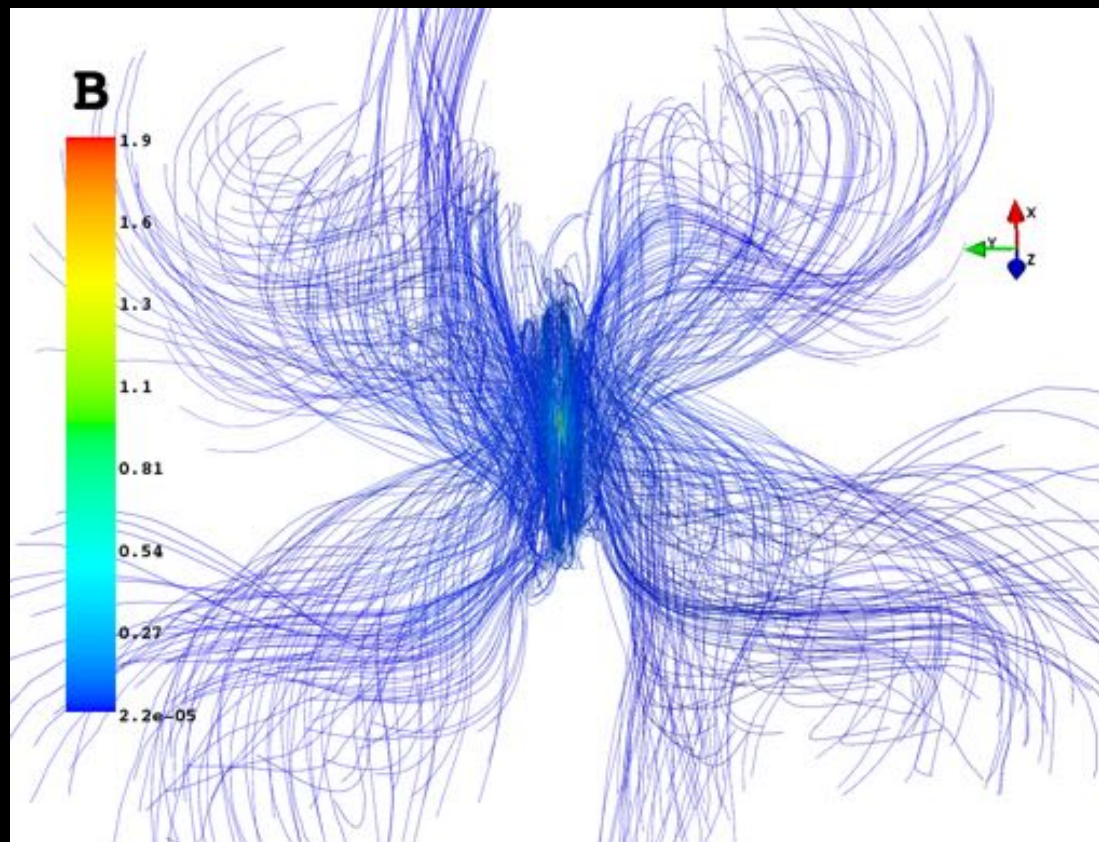
Numerical models : rotating collapsing core

Intermediate magnetisation $\lambda=5$

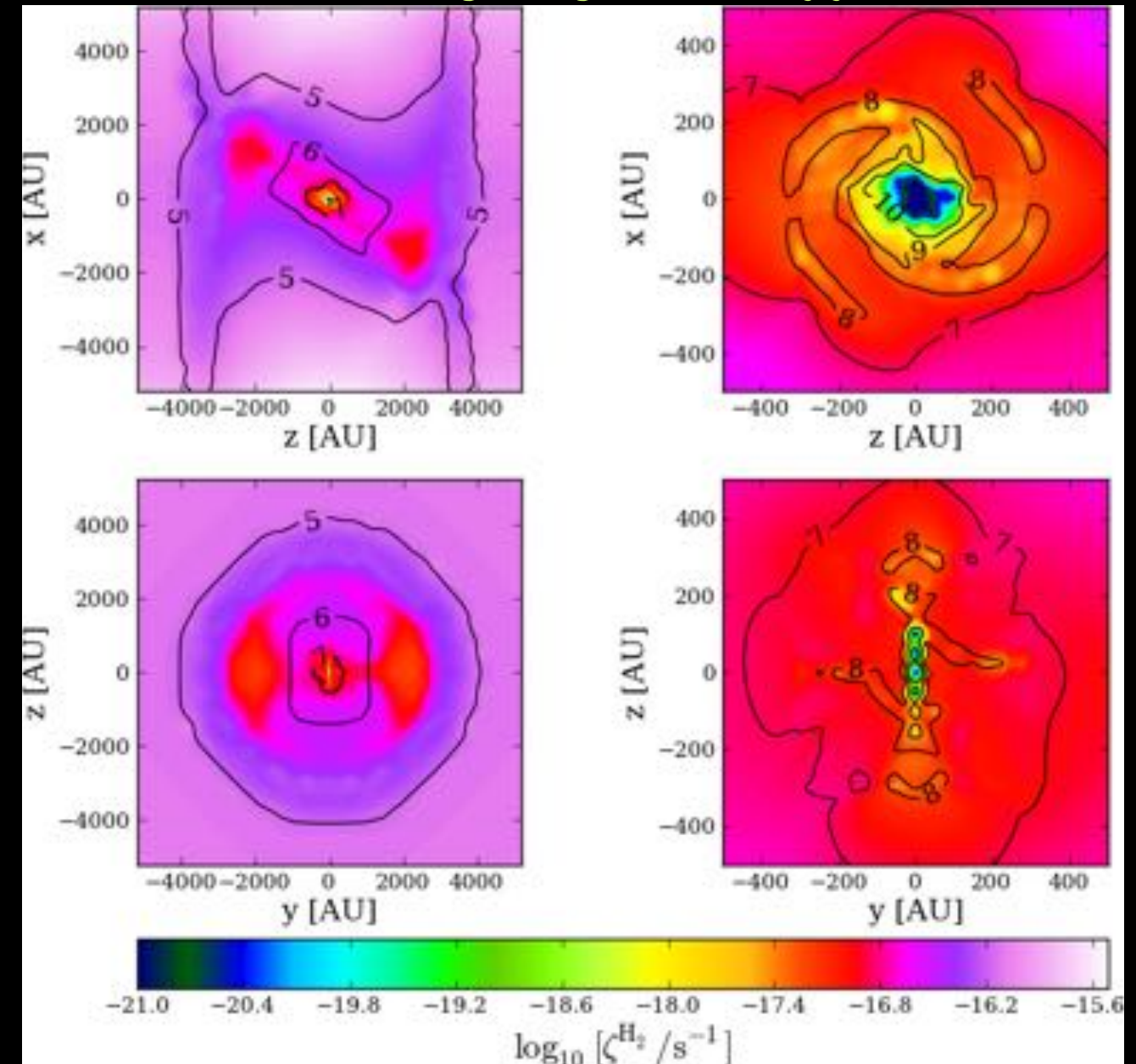
Perpendicular rotator ($J, B = \pi/2$)

$\zeta_{\text{CR}} < 10^{-18} \text{ s}^{-1}$ down to $2 \times 10^{-21} \text{ s}^{-1}$ in the inner area with an extent of a few tenths of AU. We can assume that the gas is effectively decoupled with the magnetic field.

Field lines in the inner 600 AU



including magnetic effects



Padovani+ 2013

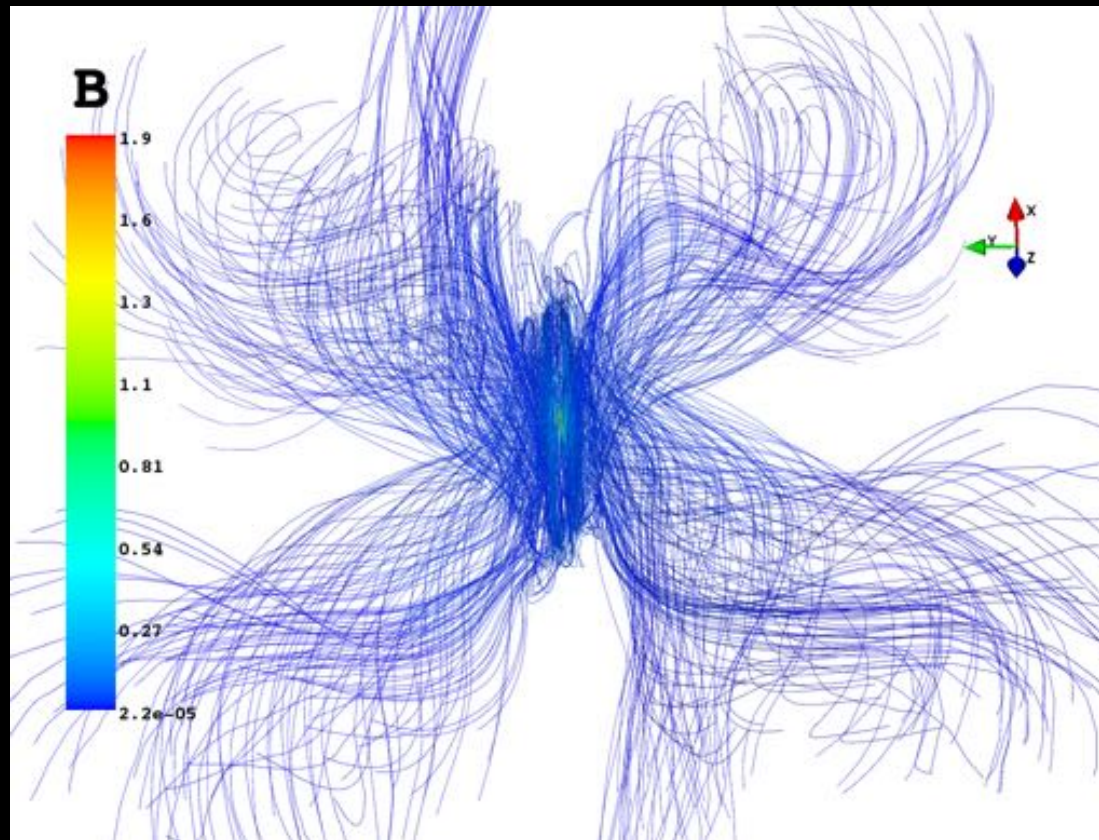
Numerical models : rotating collapsing core

Intermediate magnetisation $\lambda=5$

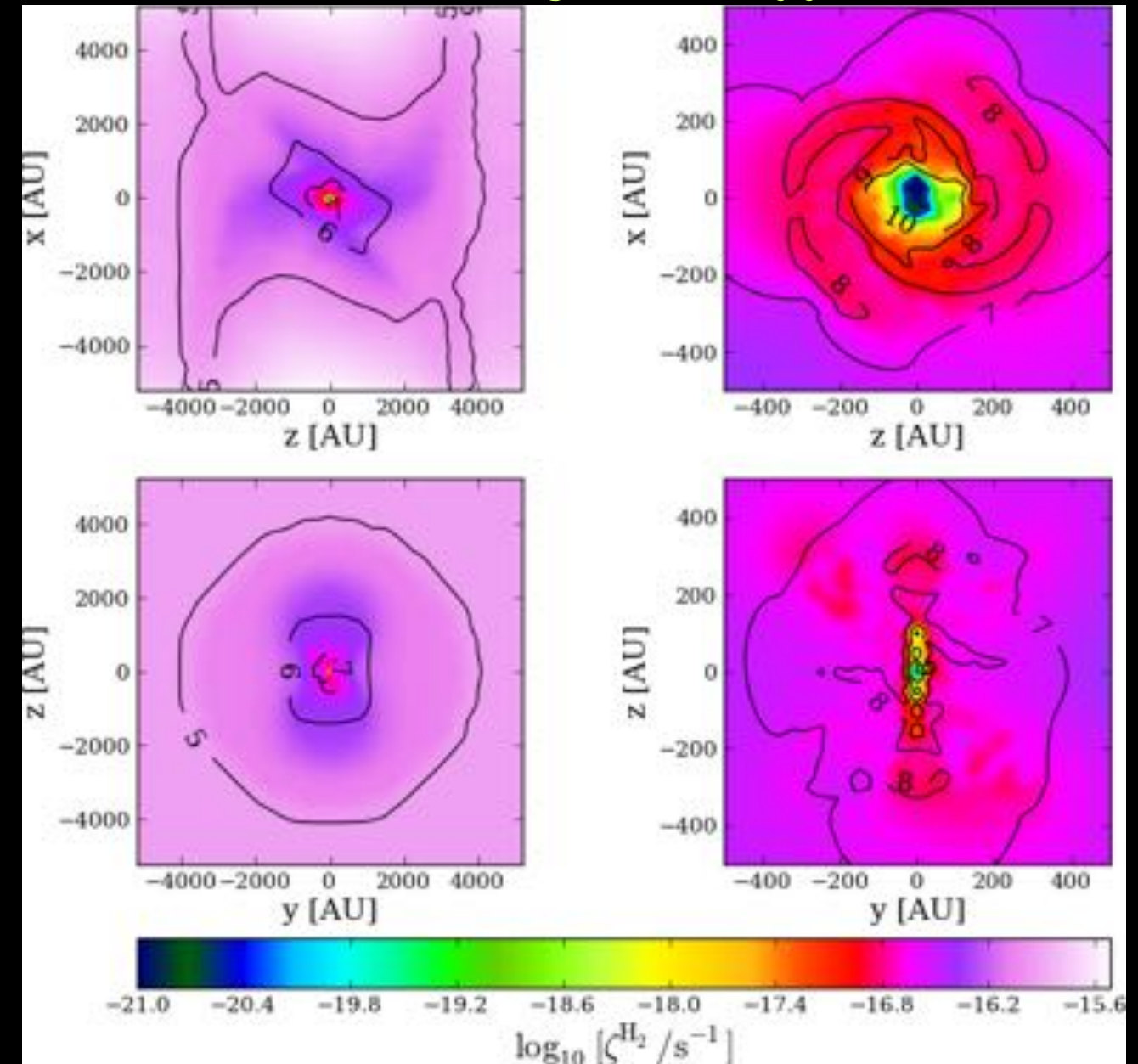
Perpendicular rotator ($J, B = \pi/2$)

$\zeta_{\text{CR}} < 10^{-18} \text{ s}^{-1}$ down to $2 \times 10^{-21} \text{ s}^{-1}$ in the inner area with an extent of a few tenths of AU. We can assume that the gas is effectively decoupled with the magnetic field.

Field lines in the inner 600 AU



without magnetic effects



Padovani+ 2013

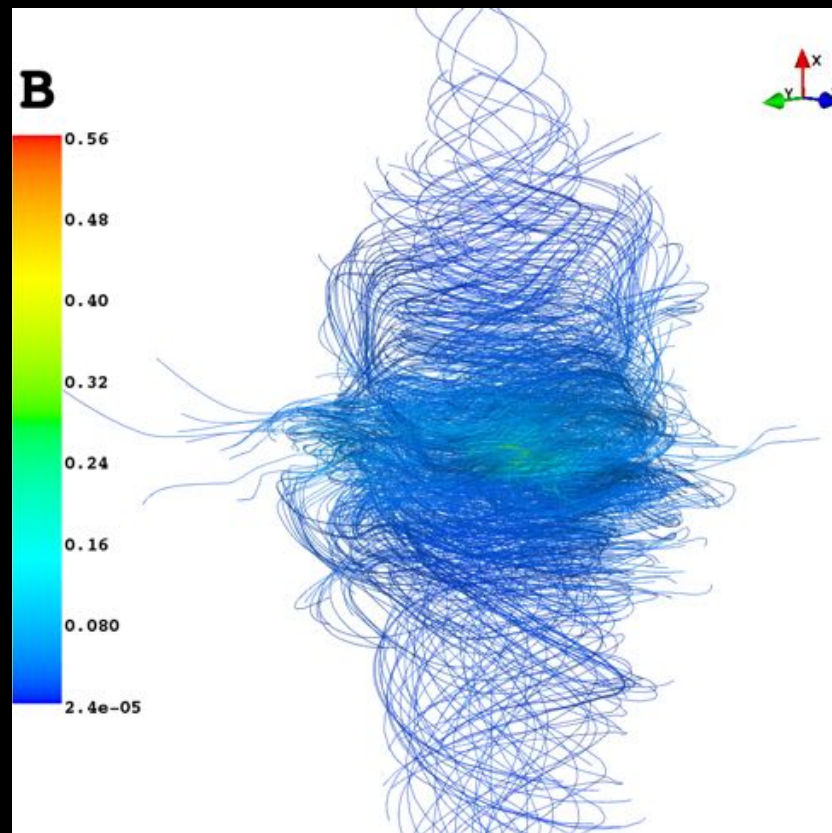
Numerical models : rotating collapsing core

Weak magnetisation $\lambda=17$

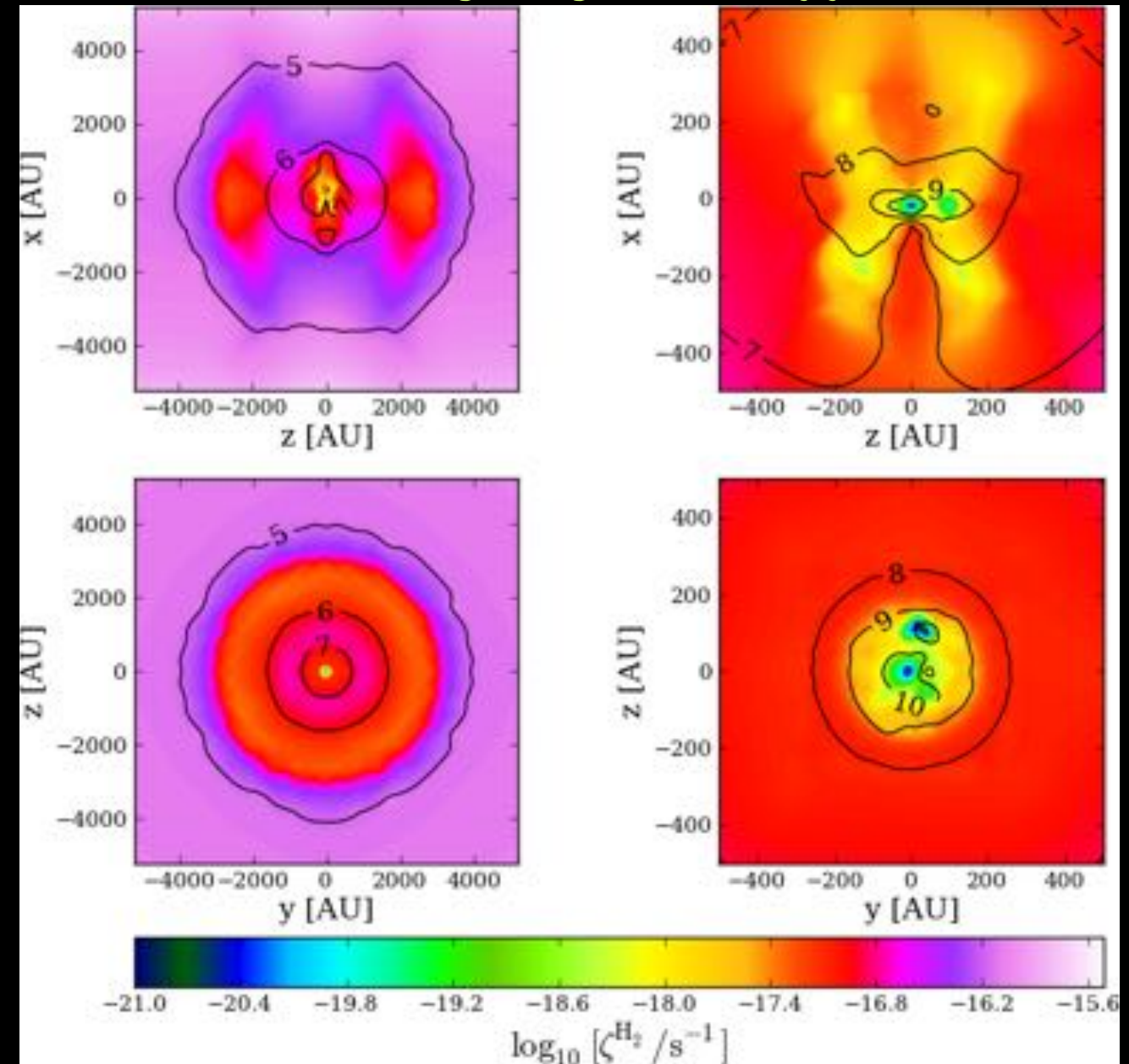
Aligned rotator (\mathbf{J}, \mathbf{B})=0

The magnetic braking is very faint and the rotation acts in wrapping powerfully the field lines. The region with $\zeta_{\text{CR}} < 10^{-18} \text{ s}^{-1}$ broadens out along the rotation axis where field line tangling up is very marked.

Field lines in the inner 600 AU



including magnetic effects



Padovani+ 2013

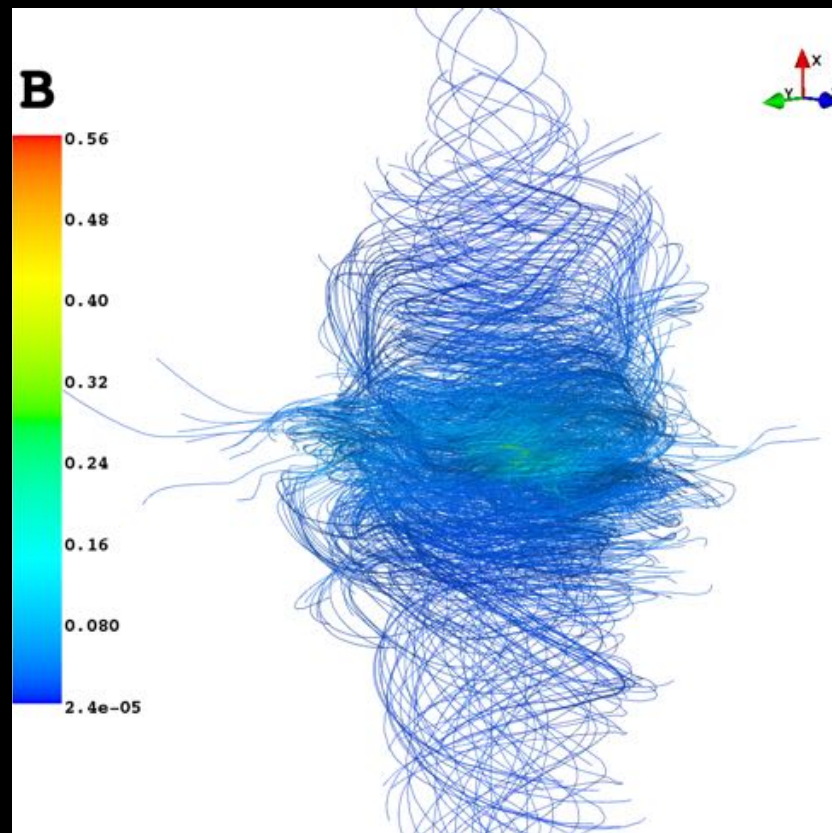
Numerical models : rotating collapsing core

Weak magnetisation $\lambda=17$

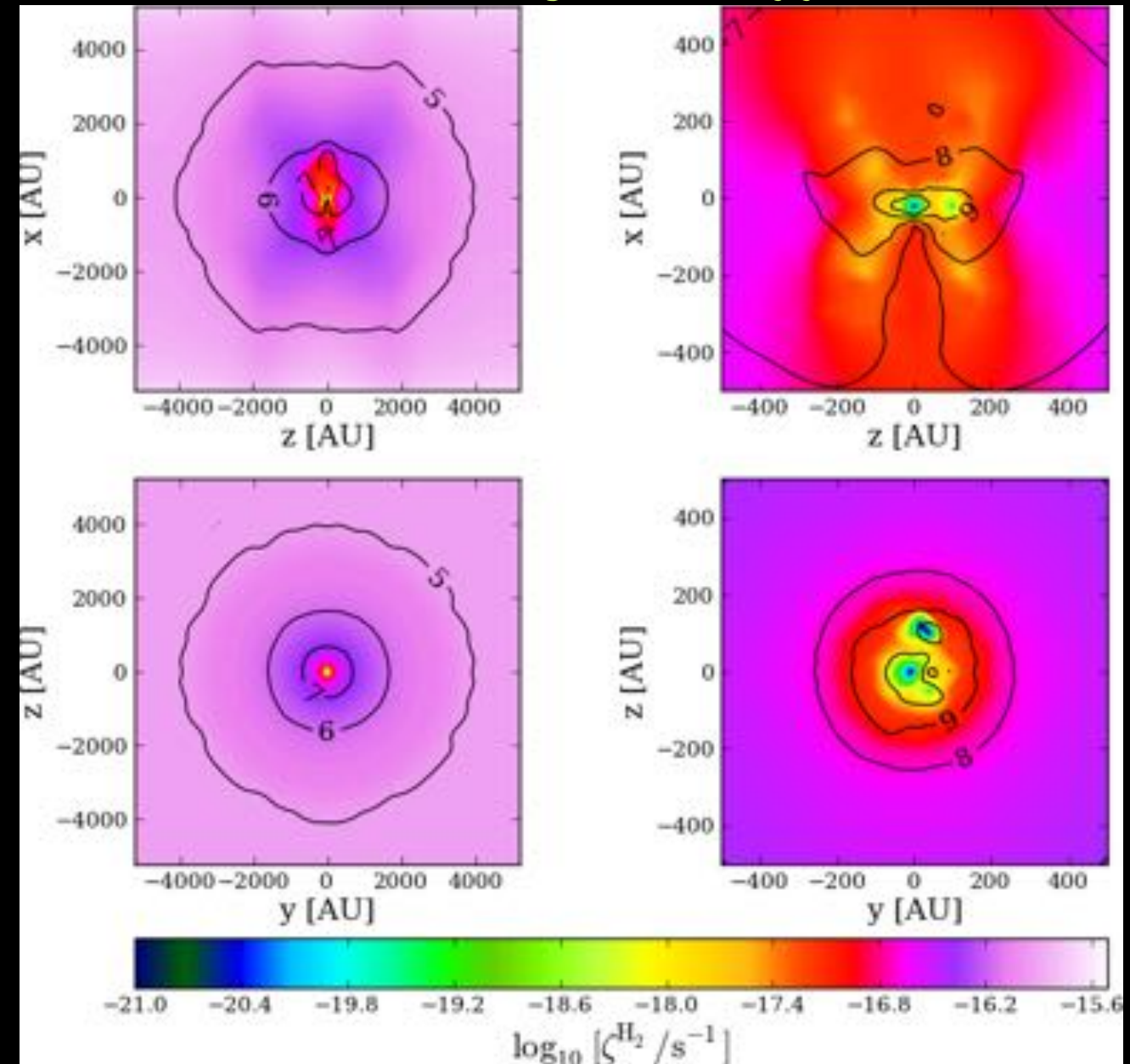
Aligned rotator (\mathbf{J}, \mathbf{B})=0

The magnetic braking is very faint and the rotation acts in wrapping powerfully the field lines. The region with $\zeta_{\text{CR}} < 10^{-18} \text{ s}^{-1}$ broadens out along the rotation axis where field line tangling up is very marked.

Field lines in the inner 600 AU



without magnetic effects



Padovani+ 2013

A useful fitting formula

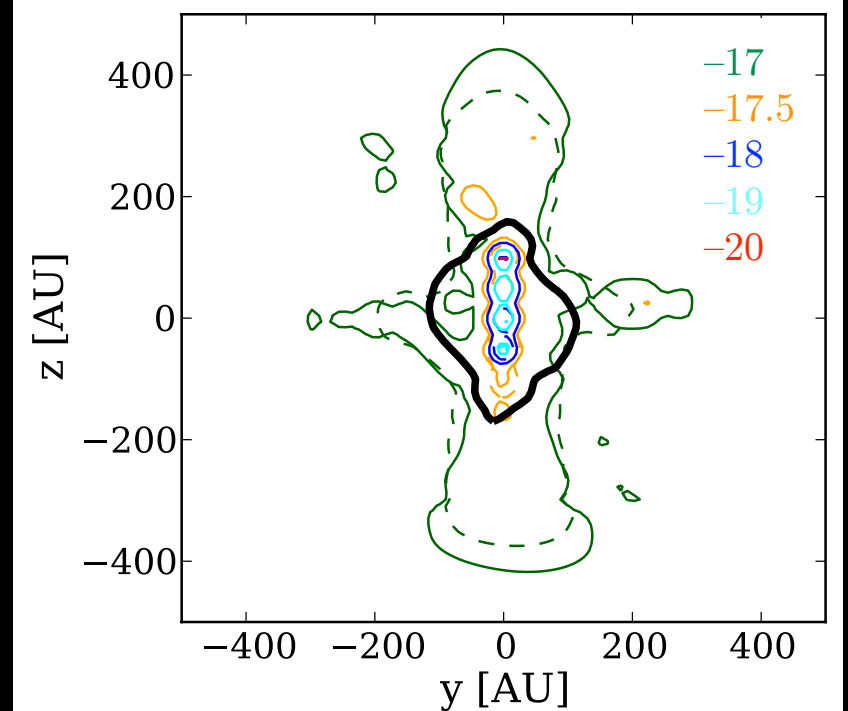
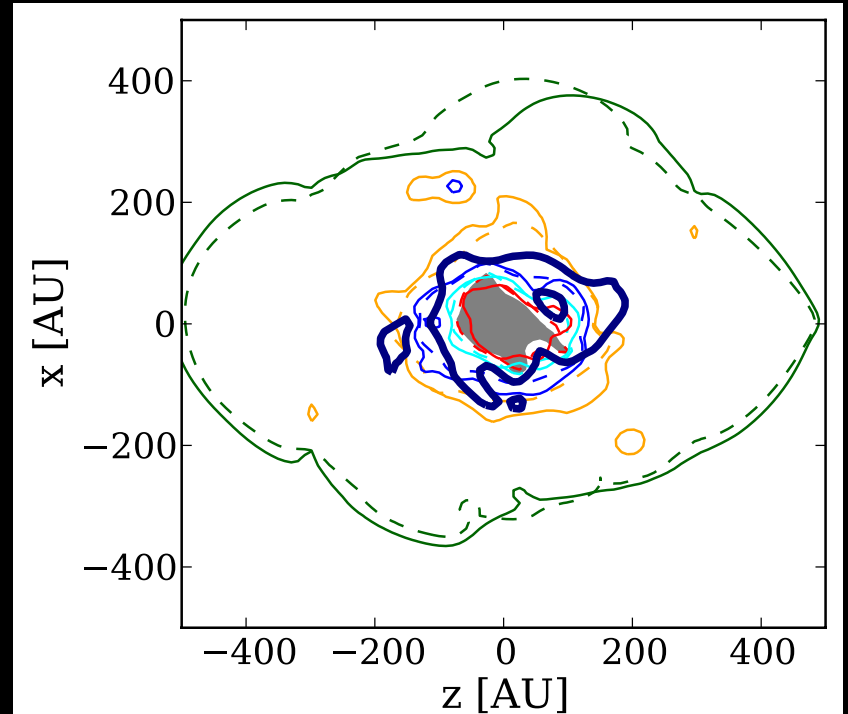
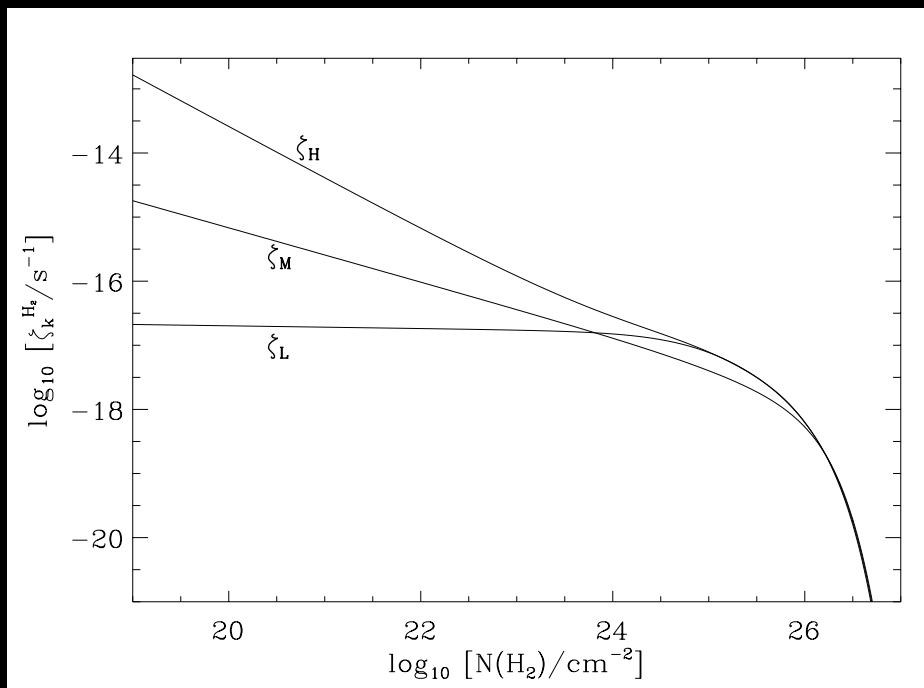
When in presence of a magnetic field, the effective column density, N_{eff} , seen by a CR can be much larger than that obtained through a rectilinear propagation.

$N(\text{H}_2)$ = average column density seen by an isotropic flux of CRs

$$N_{\text{eff}} = (1 + 2\pi \mathcal{F}^s) N(\text{H}_2)$$

$$\mathcal{F} = \mathcal{F}(|\mathbf{B}|, |B_\phi/B_p|), \quad s = s(n)$$

$$\zeta_{\text{eff}}^{\text{H}_2} \propto \zeta^{\text{H}_2}(N_{\text{eff}})$$



Cosmic rays and magnetic diffusion

(PM, Galli, Hennebelle,
Commerçon & Joos 2014)

Drifts of charged species with respect to neutrals
determines different regimes of magnetic diffusivity.

$$\frac{\partial \vec{B}}{\partial t} + \nabla \times (\vec{B} \times \vec{U}) = \nabla \times \left\{ \eta_O \nabla \times \vec{B} + \eta_H (\nabla \times \vec{B}) \times \frac{\vec{B}}{|B|} + \eta_{AD} \left[(\nabla \times \vec{B}) \times \frac{\vec{B}}{|B|} \right] \times \frac{\vec{B}}{|B|} \right\}$$

Resistivities

Conductivities

$$\left\{ \begin{array}{l} \eta_{AD} = \frac{c^2}{4\pi} \left(\frac{\sigma_P}{\sigma_P^2 + \sigma_H^2} - \frac{1}{\sigma_{||}} \right) \\ \\ \eta_H = \frac{c^2}{4\pi} \left(\frac{\sigma_H}{\sigma_P^2 + \sigma_H^2} \right) \\ \\ \eta_O = \frac{c^2}{4\pi \sigma_{||}} \end{array} \right.$$

$$\sigma_{||} = \frac{ecn(H_2)}{B} \sum_i Z_i x_i \beta_{i,H_2}$$

$$\sigma_P = \frac{ecn(H_2)}{B} \sum_i \frac{Z_i x_i \beta_{i,H_2}}{1 + \beta_{i,H_2}^2}$$

$$\sigma_H = \frac{ecn(H_2)}{B} \sum_i \frac{Z_i x_i}{1 + \beta_{i,H_2}^2}$$

The degree of diffusion is determined by the ionisation fractions that,
in turn, are determined by ζ^{H2} .

Abundance of charged species

We adopted a simplified chemical network that computes the steady-state abundance of \mathbf{H}^+ , \mathbf{H}_3^+ , a typical molecular ion $m\mathbf{H}^+$ (e.g. HCO^+), a typical metal ion M^+ (e.g. Mg^+), e^- and *dust grains* (g^0 , g^-) as a function of:

- H_2 density ;
 - Temperature ;
 - *Cosmic-ray ionisation rate.*
- }
- computed at each spatial position
in our models.

Table 1. Parameters of the simulations described in the text: non-dimensional mass-to-flux ratio λ , initial angle between the magnetic field direction and the rotation axis $\alpha_{B,J}$, time after the formation of the first Larson's core t (core formed in the centre of the pseudo-disc with $n \gtrsim 10^{10} \text{ cm}^{-3}$ and $r \sim 10 - 20 \text{ AU}$), initial mass M_{in} , mass of the protostellar core M_{\star} and of the disc M_{disc} .

Case	λ	$\alpha_{B,J}$ [rad]	t [kyr]	M_{in} [M_{\odot}]	M_{\star} [M_{\odot}]	M_{disc} [M_{\odot}]
L_1	5	0	0.824	1	—	—
L_2	5	$\pi/2$	10.756	1	0.46	0.28
H	~ 2	no initial rotation	6.000	100	1.24 ^a	0.87 ^a

^a This value refers to the densest fragment formed.

Effects of the grain size distribution

Grains play a decisive role in determining the degree of coupling between gas and B.

Three grain size distribution

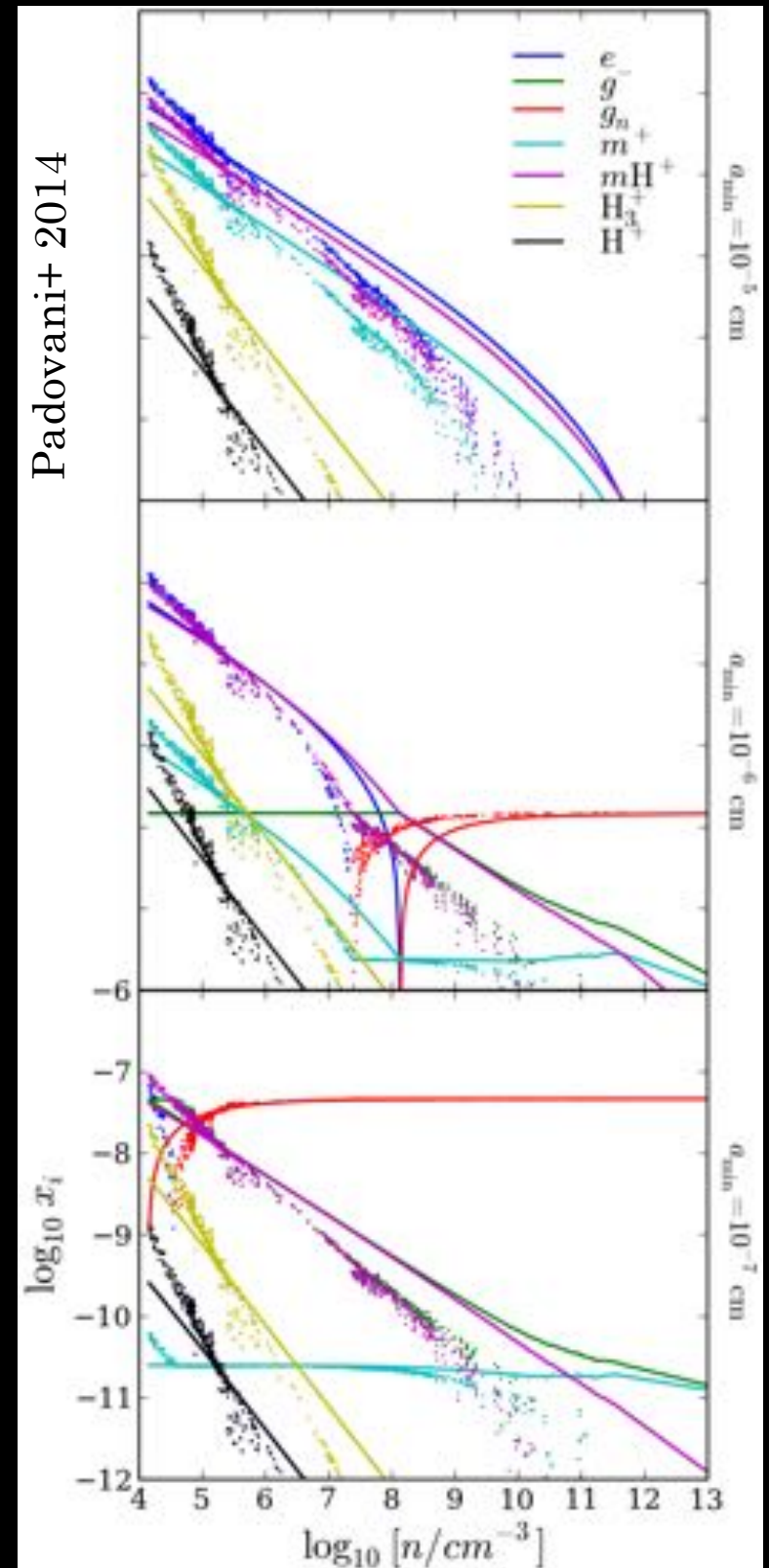
$a_{\min} = 10^{-5}$ cm (representative of large grains formed by compression and coagulation during collapse; Flower et al. 2005)

$a_{\min} = 10^{-6}$ cm (the minimum grain radius of a MRN size distribution Mathis et al. 1977 that gives the same grain opacity found by Flower et al. 2005)

$a_{\min} = 10^{-7}$ cm (typical size of very small grains)

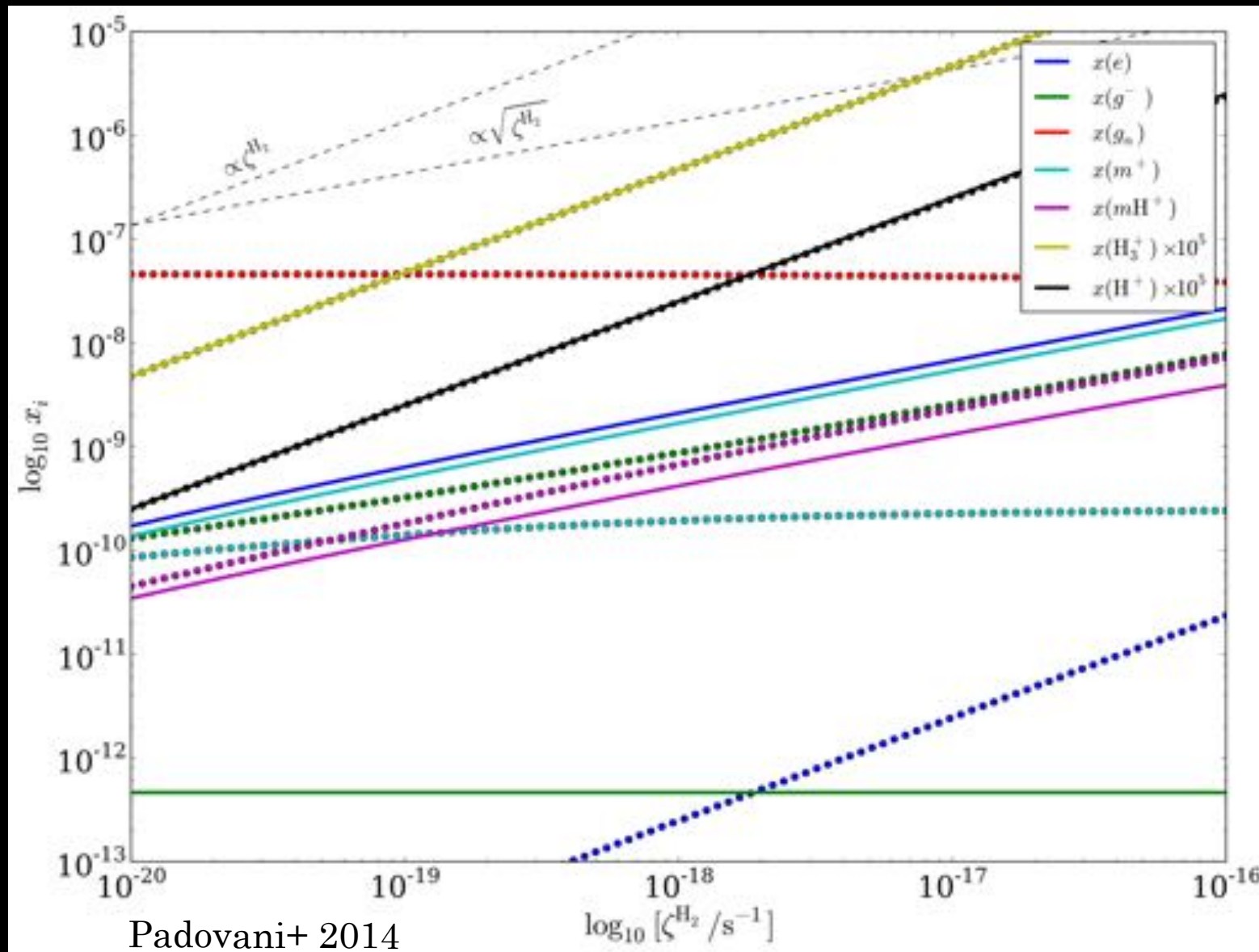
$a_{\max} = 3 \times 10^{-5}$ cm (Nakano et al. 2002)

larger grains → less number of grains
 → more free electrons (one electron per grain)



Dependence of chemical abundances on ζ^{H_2}

Density of charged species usually parameterised as $n(i) \propto (\zeta^{\text{H}_2})^{k'}$ with $k' \approx 1/2$ (e.g. Ciolek & Mouschovias 1994, 1995), but... it depends on the grain size!



$n(\text{H}_2) = 10^6 \text{ cm}^{-3}$
 $a_{\min} = 10^{-5} \text{ cm}$ (solid lines)
 $a_{\min} = 10^{-7} \text{ cm}$ (dotted lines)

k'	10^{-5}	10^{-7}
e^-	$1/2$	1
M^+	$1/2$	0
g^-	0	$1/2$
$\text{H}_3^+, \text{H}^+, m\text{H}^+$	$1/2$	$1/2$

ζ_{H_2} and the gas-magnetic field decoupling

Drift velocity of magnetic field \mathbf{U}_B : it can be represented by the velocity of the charged species (frozen with the field lines) with respect to neutrals.

By comparing \mathbf{U}_B with the fluid velocity, it is possible:

- to assess the degree of diffusion of the field;
- to estimate the size of the region where gas and B are decoupled.

Following Nakano et al. (2002), \mathbf{U}_B can be written as a function of the resistivities.

$$\vec{U}_B = \vec{U}_{\text{AD}} + \vec{U}_{\text{H}} + \vec{U}_{\text{O}} = \frac{4\pi}{cB^2} \left[(\eta_{\text{AD}} + \eta_{\text{O}}) \vec{j} \times \vec{B} + \eta_{\text{H}} (\vec{j} \times \vec{B}) \times \frac{\vec{B}}{B} \right]$$

$$\frac{1}{t_B} = \frac{1}{t_{\text{AD}}} + \frac{1}{t_{\text{H}}} + \frac{1}{t_{\text{O}}}$$

$$t_k = R/U_k, \quad (k = \text{AD, H, O})$$

R is the typical length scale of the region
(assumed as the distance from the density peak)

ζ_{H_2} and the gas-magnetic field decoupling

$$\frac{1}{t_B} = \frac{1}{t_{\text{AD}}} + \frac{1}{t_{\text{H}}} + \frac{1}{t_{\text{O}}}$$

$$t_k = R/U_k, \quad (k = \text{AD, H, O})$$

R is the typical length scale of the region
(assumed as the distance from the density peak)

Nakano et al. (2002): comparison between t_B and the free-fall time scale.
Here we compare t_B with the $t_{\text{dyn}} = R/U$ (U = fluid velocity including infall and rotation).

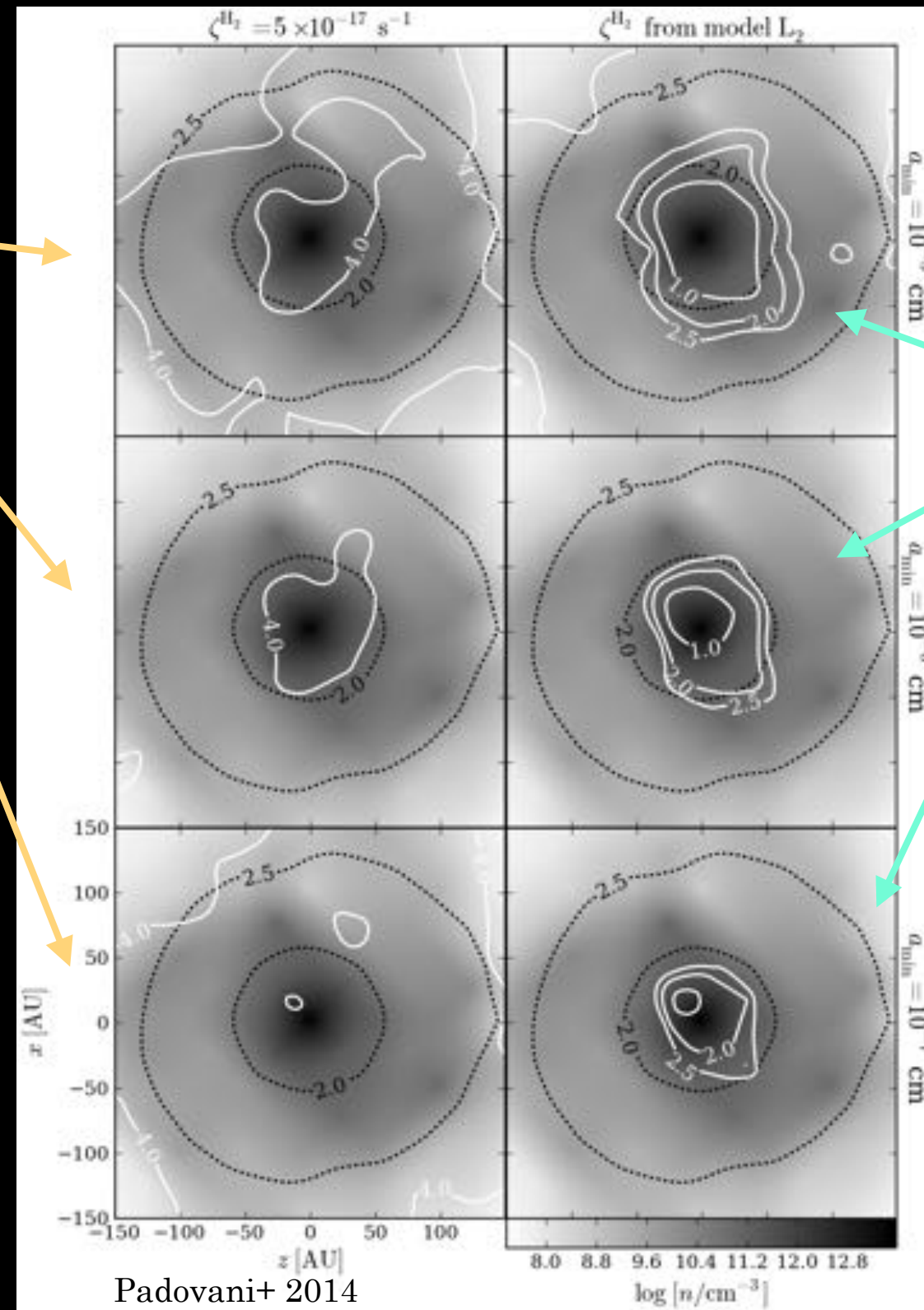
In regions where:

- $t_B < t_{\text{dyn}}$: B is partially decoupled and it has less influence on gas dynamics;
- $t_B > t_{\text{dyn}}$: diffusion is not efficient and B remains well coupled to the gas.

Is there a relevant variation in t_B using a constant $\zeta^{\text{H}_2} \approx 10^{-17} \text{ s}^{-1}$ or accounting correctly for the dependence of ζ^{H_2} on $N(\text{H}_2)$ and B ?

YES!

$t_B > t_{\text{dyn}}$



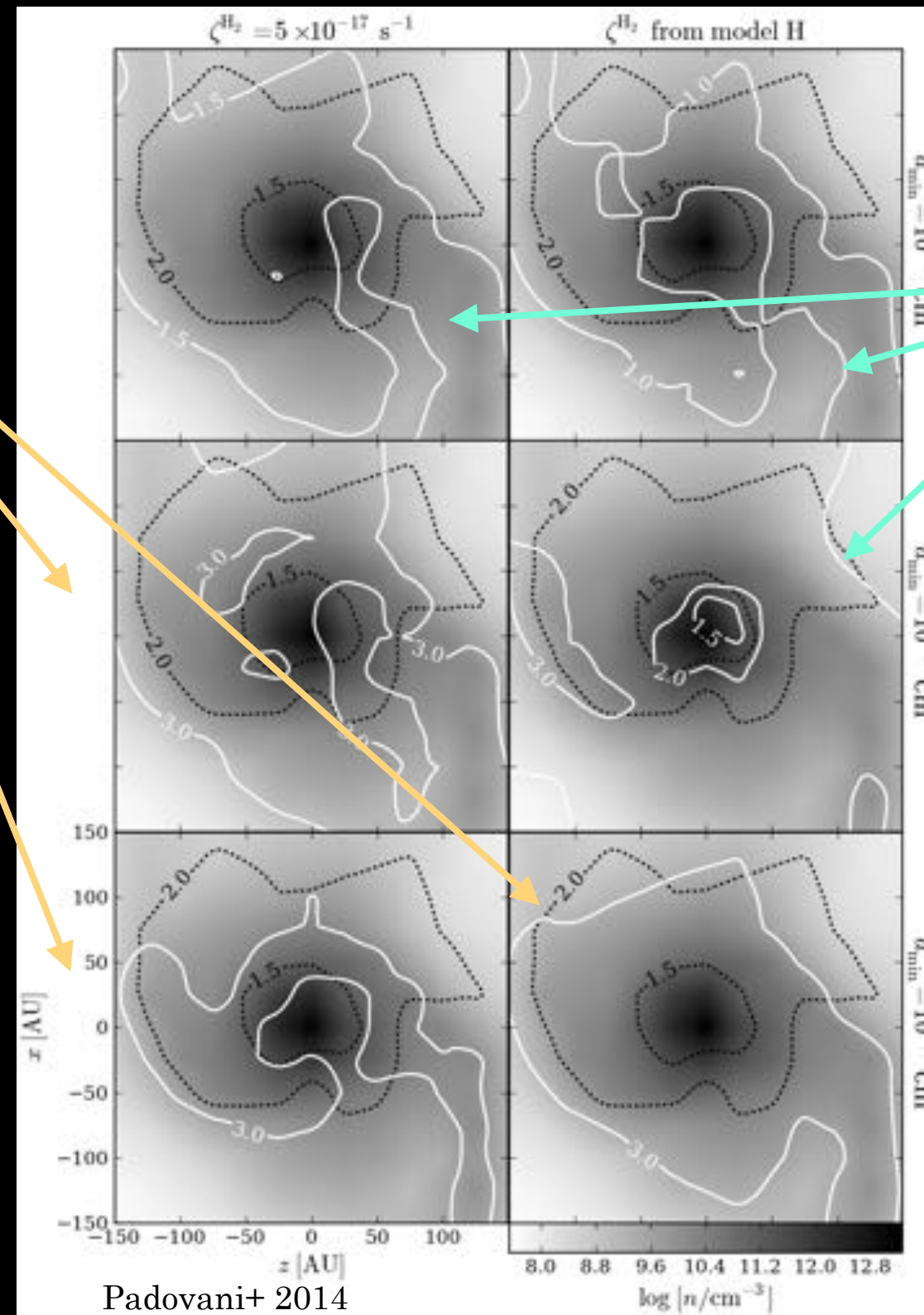
Cosmic-ray ionisation rate and diffusion time scale LOW-MASS CASE

$t_B < t_{\text{dyn}}$

The region of decoupling decreases with decreasing a_{min} (from ≈ 50 AU to ≈ 20 AU of radius), but it is still present.

The correct evaluation of the CR ionisation rate as a function of density and magnetic field allows the diffusion time to decrease up to three order of magnitudes.

$t_B > t_{\text{dyn}}$



Cosmic-ray ionisation rate and diffusion time scale HIGH-MASS CASE

$t_B < t_{\text{dyn}}$

For $a_{\min} = 10^{-5} \text{ cm}$ the decoupling region has a radius of $\approx 100 \text{ AU}$, but for $a_{\min} = 10^{-7} \text{ cm}$ it vanishes.

Different behaviour wrt low-mass case:
the field diffuses faster in the HM case
(turbulent nature of the flow).
Problems with limited resolution?
Numerical diffusion (Hennebelle+ 2013;
Joos+ 2013).

The turbulent diffusion present in the
HM model reduces the field strength
making the microscopic resistivities
smaller (no decoupling).

Conclusions

- The study of **low energy** ($E < 1$ GeV) cosmic rays is fundamental for correctly dealing with **chemical modelling** and **non-ideal MHD simulations**;
- In order to study the cosmic-ray propagation we accounted for **energy losses** and **magnetic field effects**: an increment of the toroidal component, and in general a **more tangled magnetic field**, corresponds to a **decrease of ζ_{H2}** because of the growing preponderance of the **mirroring effect**;
- The extent to which density and magnetic effects make ζ_{H2} decrease can be ascribed to the degree of magnetisation; $\zeta_{H2} < 10^{-18} \text{ s}^{-1}$ is attained in the central **300-400 AU**, where $n > 10^9 \text{ cm}^{-3}$, for toroidal fields larger than about **40%** of the total field in the cases of intermediate and low magnetisation (**$\lambda=5$ and 17** , respectively);
- We found an increase in η in the innermost region of a cloud after the collapse onset: (1) field has to be considerably twisted; (2) dust grains had time to grow by coagulation.

A correct treatment of CR propagation can explain the occurrence of a decoupling region between gas and magnetic field that in turn affects the disc formation.